Dehydration of Methanol to Dimethyl ether, Ethylene and Propylene over Silica-Doped Sulfated Zirconia

Syed T. Hussain,[*] M. Mazhar, Sheraz Gul, Karl T Chuang,[†] and Alan R. Sanger[†]

Department of Chemistry, Quaid-e-Azam University, Islamabad 45320, Pakistan. [*]E-mail: dr_tajammul@yahoo.ca
[†]Department of Chemical Engineering, University of Alberta, Alberta, Canada T6G 2G6

Two types of catalyst samples were prepared, one sulfated zirconia and the other silica doped sulfated zirconia. The acidity tests indicate that sulfated zirconia doped with silica has higher concentration and strength of acidic catalyst sites than undoped sulfated zirconia. The acidic surface sites have been characterized using FTIR, NMR, pyridine adsorption, TPD, XRD and nitrogen adsorption. Doping with silica increased the concentration of surface Lewis and Brønsted acid sites and resulted in generation of proximate acid sites. The activity test indicates that doping sulfated zirconia with silica increases both the acidity and catalytic activity for liquid phase dehydration of methanol at 413-453 K. Methanol is sequentially dehydrated to dimethyl ether and ethylene over both catalysts. Significant amounts of propylene are also formed over the silica-doped catalyst, but not over the undoped catalyst.

Key Words : Sulfated zirconia, Dehydration of methanol, Dimethyl ether, Ethylene, Propylene

Introduction

Solid acid catalysts play an important role in hydrocarbon conversion reactions in the petroleum and chemical industries.[1] In particular, the solid super-acid properties and activity of sulfated zirconia were first described over a decade ago,[2] which led to intense research in this area. Rational design of solid acid catalysts for a specific application requires control of acid site type (Lewis, Brønsted), density, and strength. To this end, there are two general strategies for modification of the acidic properties of catalytic oxides. One approach is to dope the oxide with anions. Anionic dopants can increase the electron-withdrawing capability of the doped surface, thereby enhancing the ability of neighboring hydroxyl groups to act as proton donors. A second approach is to dope an oxide catalyst with a second oxide. Modeling of the performance and acidity of mixed oxides show that strongly acidic sites form when large localized charge imbalances develop at M-O-M' linkages (M and M' are different cations).[3,4] The high catalytic activity of sulfated zirconia has been attributed to super-acidity.[5-7]

The goal of the present research is formulation of highly active acidic catalytic materials. To this end we are preparing, characterizing and testing modified zirconium sulfate based catalysts having Lewis and Brønsted acid sites with different concentrations and strengths. We have now found that doping zirconium sulfate with silica increases both the strength and density of surface acidic sites, and their catalytic activity. Herein we will compare the catalytic activity of silica-doped sulfated zirconia (SZS) with that of undoped sulfated zirconia (SZ) using, as a probe reaction, methanol dehydration to sequentially form dimethyl ether and ethylene. We will show that significant amounts of propylene are also formed when the catalyst is SZS, but not when it is SZ. A detailed comparison of the physical properties of SZS and SZ and the respective surface acidic sites using spectroscopic and microscopic techniques and chemical probes has also been described.

Experimental Details

Catalyst Preparation. Zirconium oxynitrate [$ZrO(NO_3)_2$] was dissolved in 10 N nitric acid solution. Aqueous ammonia was then slowly added to the stirred solution to precipitate zirconium hydroxide, until the pH was *ca.* 11. The precipitate was recovered by filtration, washed with water and calcined at 573 K for 4 hours under atmospheric conditions to form zirconia.

Sulfated zirconia (SZ) was prepared by suspending 5 g zirconia in 100 mL of an aqueous solution containing 50 wt% sulfuric acid. The solution was then heated to evaporate water using a hotplate. The solid formed by drying the mixture over the hot plate for *ca.* 2 h was calcined at 923 K for 4 hours under atmospheric conditions.

Silica-doped sulfated zirconia (SZS) was prepared using substantially the same procedure as described above, except that a weighed amount of silica was added to the stirred reaction mixture before heating.

Catalyst Characterization. BET surface areas of fresh and used catalysts were determined by nitrogen adsorption at 77 K (Table 1). Crystallite sizes of fresh and used samples were determined using the Scherer equation and presented in Table 2. Pyridine adsorption was used to determine the acidic sites using FTIR, TPD and NMR and then their consequent effect on the catalytic activity was discussed.

The amount of sulfate leached from SZ or SZS during catalytic tests was determined by acid-base titration of the residual liquid reaction mixture.

Catalytic Activity Testing. Reactions were performed in

Table 1. BET area and pore volume for fresh and used catalysts

Catalyst sample	Surface area m^2/g (Fresh)	Surface area m^2/g (Used)	Pore Volume mL/g (Fresh)	Pore Volume mL/g (Used)
SZ	191.58	146.83	0.1082	0.1744
SZS	223.14	172.98	0.09231	0.1443

Table 2. Crystallite size (XRD data)

Catalyst sample	Crystallite size (nm) (Fresh)	Crystallite size (nm) (Used)
SZ	14.60	31.5
SZS	13.60	30.0

a batch slurry reactor system (Figure 1). The reactor was a high pressure SS-316 reactor with a volume of 320 mL (model 4841, Parr Instruments Inc. USA), equipped with an impeller. A J-type thermocouple was immersed into the liquid phase to measure the reactor temperature, and was connected to a heater/controller to maintain the reactor temperature within ± 1 K. Liquid samples were collected using a 1/8 inch o.d. stainless steel tube connected to a stainless steel sampling valve. A pressure transducer (Foxboro electronic transmitter, Model 84 GM-D) was used to measure pressure in the reactor with an accuracy of ± 4.0 kPa.

Analyses of Reaction Mixtures. Liquid and gas samples were analyzed using a Hewlett Packard 5890 Series II Gas Chromatograph (GC) equipped with a TCD detector and a 0.914 m long column with Poropak R packing (50-80 mesh), operated at a constant column temperature of 423 K.

The GC was calibrated for ethylene, propylene, dimethyl ether (DME), water and methanol using standard mixtures having different concentrations of ethylene, propylene and dimethyl ether (DME). The exit gasses were analyzed for DME, ethylene and propylene.

Liquid samples (1 mL) were taken hourly and analyzed using GC. Analyses of the vapor phase were performed online. Compositions of gas and liquid phase product mixtures were determined by comparison of GC data with

Figure 1. Schematic diagram of the equipment.

standard mixtures.

Procedure. First, 150 mL of methanol (analytical grade, BDH) and 2.0 g of catalyst were loaded into the reactor, so that initially about one half of the vessel was filled with liquid. The liquid expanded at high temperatures; hence space was allocated to accommodate this expansion. The reactor was then purged with helium to remove any air initially present in the reactor, and to provide an inert atmosphere. The inlet and outlet of the reactor were then closed. The amount of helium initially present in the reactor prior to heating was determined from the initial reactor temperature, pressure and vapor volume after sealing the reactor, and was used as an internal standard to calculate material balance in kinetic studies.

The reactor contents were then heated to a reaction temperature pre-selected from 373, 413, 433 and 453 K. The range 373-453 K was selected for two reasons. First, the reaction rate was sufficiently fast to allow experiments to be completed within hours. Second, pressures developed within this range could be reproducibly determined with good accuracy using the present experimental equipment. The pressure in the closed reactor rose from 260 psig at 413 K to 375 psig at 433 K and 575 psig at 453 K. The temperature range 413-453 K was then selected for more detailed investigation because a significant amount of alkene reaction product was produced in this range.

Negligible amounts of reaction products were produced during the time required to heat the reaction mixture to the pre-selected temperature as monitored by on line GC during the ramp.

The reaction mixture was stirred at 1080 rpm for the duration of the reaction (1-3 hours) to minimize the influence of external mass transfer. Selectivity and conversion were calculated from GC analytical results.

After the reaction, the residual product liquid was filtered and the catalyst was recovered, dried and could be used again for further reaction.

Catalyst Characterization Using XRD and BET. The increase in surface area of fresh SZS compared to fresh SZ was attributed to modification of the catalyst structure as a consequence of doping with silica. SZS had a higher surface area than SZ, but had a slightly smaller pore volume. Doping SZ with silica reduced the average pore size.

Figure 2 shows the crystalline XRD for fresh and used samples of SZS and SZ, respectively. The XRD data showed that the physical structure of SZS differed from that of SZ.

Comparison of the XRD of fresh and used samples of each catalyst showed that the structure of SZS was more stable than that of SZ. The XRD of SZS showed much more intense peaks for 2θ at 30° and 34° in comparison with SZ. This suggested that SiO$_2$ doping not only resulted in a more stable crystal structure, but also in modification of catalyst physical characteristics (Figure 2b). The differences between the XRD data for the two fresh samples were consistent with a combination of a change in crystal structure resulting from doping SZ with SiO$_2$, and a minor change in size of crystallites. There were similar differences between used samples

(a) SZS: fresh (F) and used (U) catalysts

(b) SZ: fresh (F) and used (U) catalysts
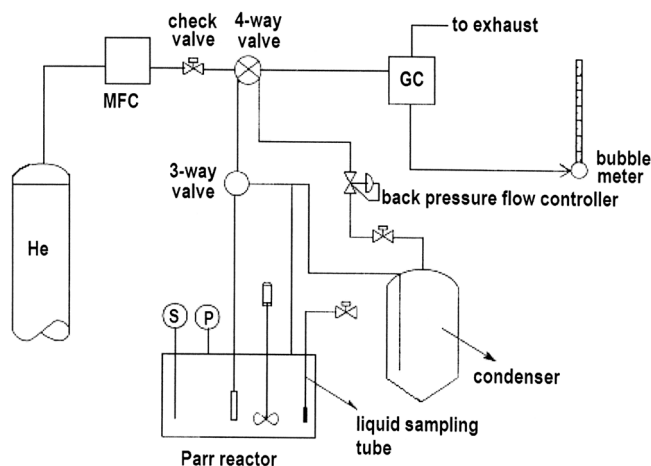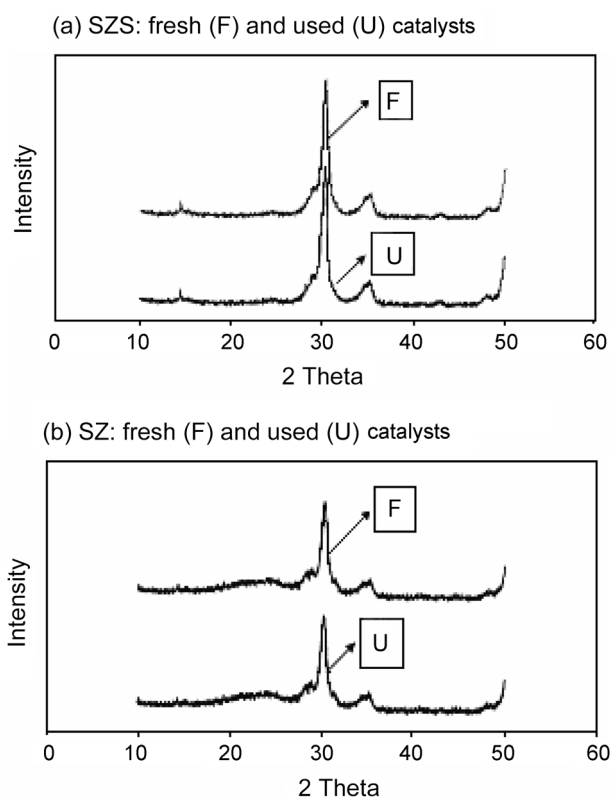
Figure 2. XRD spectra of fresh and used samples of (a) silica doped and (b) undoped sulfated zirconia.

(a) Before pyridine adsorption

(b) After pyridine adsorption

Figure 3. FTIR spectra of undoped and silica doped catalysts before and after adsorption of pyridine.

of SZ and SZS. However, the surface areas and crystallite sizes of used SZ and SZS were both significantly larger than those for fresh catalysts. The combination of an increase in crystallite size, coupled with an increase in surface area during the methanol dehydration reaction, suggested that the crystallites agglomerated and became more porous during the reaction. Although the cause for this combination of effects cannot be determined unambiguously from the present data, it may in part have been a consequence of leaching of a portion of sulfate during that reaction. From data and Figure 2 it can be seen that the catalyst phase, surface area, pore volume and crystallite size changed appreciably during use as a catalyst for methanol dehydration. However, the changes did not appear to affect catalytic activity or selectivity when the catalyst was used in one or more catalyst runs up to 3 h in duration. The data suggest that the changes in the catalyst structure did not significantly affect catalyst sites, and that the catalysts had acceptable physical stability. The amount of sulfate ions leached over the period of the methanol dehydration experiments was not sufficient to induce any major change in the catalyst sites on SZ and SZS catalysts over a small number of runs. However, prolonged leaching resulted in catalyst deactivation. It is noteworthy that the crystal stability of SZS was greater than that for SZ (XRD, Figure 2), and the amount of sulfate leached from SZS was less than that from SZ.

The combination of the above results indicated that both the stability of active sites and the crystal structures of SZ

and SZS depended on retention of a significant portion of the original sulfate content.

Pyridine Adsorption. Typical IR spectra obtained before and after pyridine adsorption on SZ and SZS samples at 100 °C are presented in Figure 3a (before pyridine adsorption) and 3b (after pyridine adsorption). Two diagnostic peaks characteristic of pyridine interacting with Brønsted acid sites to form pyridinium ions (PyH$^+$) were observed at 1540 cm^{-1} and 1445 cm^{-1}. Additional peaks assigned to PyH$^+$ were located at 1630 cm^{-1}, 1600 cm^{-1} and 1489 cm^{-1}. Peaks at 1637 cm^{-1} and 1488 cm^{-1} have been attributed to pyridine molecules adsorbed on Lewis acid sites. Other peak observed in the spectra corresponded to physisorbed pyridine and pyridine that was hydrogen-bonded to silanol groups.

The spectrum for pyridine adsorbed on SZS (Figure 3b) showed an intense pyridinium (PyH$^+$) peak at 1445 cm^{-1}. Thus, SZS had a higher concentration of Brønsted acid sites than SZ. However, only small shoulders were observed at 1488 and 1637 cm^{-1}, that corresponded to a trace amount of pyridine adsorbed at Lewis acid sites. When the sample was exposed to further pyridine, only the peaks at 1445 and 1637 cm^{-1} increased in intensity, indicating that the Brønsted and Lewis acid sites were already saturated. The intensities of the peaks at 1445 cm^{-1} and at 1637 cm^{-1} were used to estimate the concentration of the respective sites. The breadth of the FWHM [full width half maximum] of peaks at 1445, 1530 and 1630 cm^{-1} indicated the presence of additional multiple acid sites that were distinct from both of
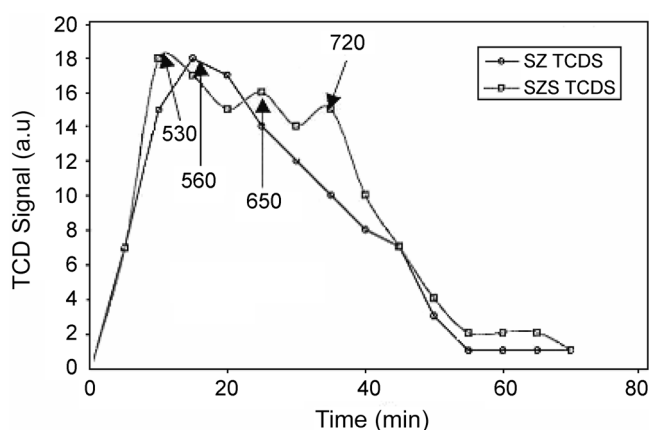
Figure 4. Temperature programmed desorption (TPD) of pyridine pre-adsorbed on undoped and silica-doped catalysts (numbers are temperature (K) corresponding to maxima).

Figure 5. FTIR analysis of spent SZS sample.

isolated Brønsted and Lewis acid sites. Both the IR peak at 1375 cm^{-1} and a ^{1}H NMR signal at 5.75 ppm, assigned to super-acid protons, lost intensity after pyridine adsorption.

Thus, Brønsted, Lewis and combinations of proximate acid sites were all available as potentially active acidic catalyst sites.

The concentration of Brønsted acid sites determined for the SZS sample, in accordance with the method of reference,[8] was found to be 1.1×10^{20} ions.g^{-1}. Both SZ and SZS samples displayed a prominent feature (Figure 3a) at 1375 cm^{-1}, arising from increased S=O double bond character for sulfate ions at high temperature.

Temperature Programmed Desorption of Pyridine. Figure 4 shows the TPD of pyridine on SZ and SZS. It was found that the strength of adsorption of pyridine on SZS was higher than on SZ. SZ did not adsorb pyridine at Brønsted acid sites at 423 K. The acidity of Brønsted acid sites of SZS was stronger after activation at 923 K.

The TPD of pyridine on SZS displayed two features at 650 and 720 K that were not present in TPD of pyridine on SZ. Detection of these additional features indicated that combinations of proximate acid sites were present only on SZS. In addition, SZS was found to have a higher total acid sties density, 2.4 mmol·m^{-2}, compared with 1.8 mmol·m^{-2} on SZ. Thus, the overall concentration of surface acidic sites, their strengths, and the distribution of types of site were all enhanced by doping SZ with silica to form SZS.

Characterization of Acid Sites Using NMR. ^{1}H NMR data of SZ and SZS before and after pyridine adsorption are presented in Table 5. Three distinct NMR resonances were detected, one at 5.75 ppm and two other signals at 2.1 and 1.2 ppm. The signal at 5.75 ppm was in the range attributable to super-acid protons. The intensity of the signal at 5.75 ppm was much more in the spectrum of SZS when compared with the spectrum of SZ, indicating that the concentration of strongly acid sites was higher on SZS.

Pyridine adsorption on either SZ or SZS reduced the intensity of the signal at 5.75 ppm. The reduction in intensity was greater for SZ than for SZS (Table 5). The spectrum of
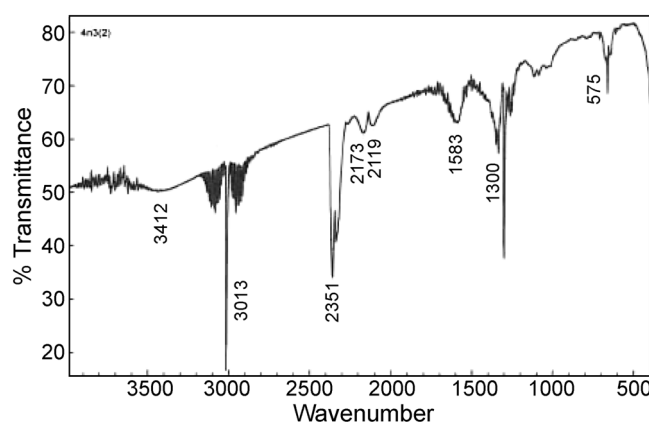
SZS treated with pyridine showed a new signal at 1.9 ppm that was assigned to pyridine adsorption at a combination of proximate acid sites. Together with the FTIR and TPD data above, the NMR data supported the proposal that SZS catalyst had complex proximate acid sites in addition to Brønsted and Lewis acid sites, and that these complex sites on SZS were more acidic than the acid sites on SZ.

Results and Discussions

Methanol dehydration was used as a model reaction for comparing the catalytic properties of SZ and SZS for reactions in the temperature range 373-453 K. The results are presented in Table 3. Methanol was dehydrated to DME at all temperatures 373-453 K over either SZ or SZS. Ethylene and propylene were produced only in reactions at 413-453 K. Formation of propylene occurred only over SZS catalyst. No other hydrocarbon products were detected.

Dehydration of Methanol to DME. Direct dehydration of methanol produced DME as the sole primary product at 373-453 K (Eq. 1). When alkenes were formed as secondary products, the concentration of DME did not increase linearly with time, as it was consumed to form ethylene or propylene.

$$2CH_3OH \longrightarrow (CH_3)_2O + H_2O \qquad (1)$$
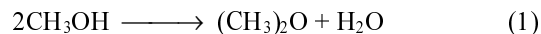
Table 3 shows the compositions of the reaction mixture after reaction for 1-3 h at different temperatures. Conversion to dehydration products over SZS catalyst was higher at all temperatures than reaction over SZ. This effect showed that the acidity of SZS was higher than that of SZ.

Dehydration of DME to Ethylene. Conversion of DME to ethylene was a secondary reaction (Eq. 2; * represents a surface site). The characteristics of catalytic sites for conversion of alcohols to olefins have been studied intensely. The mechanism for elimination of water from a C$_{2+}$ alcohol, in which the C-C bond already exists, differs from dehydration of methanol to ethylene, or to propylene. Nevertheless, similar intermediates may be formed at the catalyst surface, and so studies of conversion of aliphatic primary C$_{2+}$ alcohols to olefins on catalysts possessing acidic centers provide useful insights.[9-11] It is well known that Brønsted

Table 3. Methanol conversion and product distribution over SZ and SZS catalysts as a function of temperature

Reaction temp. (K)	Methanol conversion (%)	Product selectivity (%)		
		Dimethyl ether	Ethene	Propene
Over SZ catalyst				
413	32.5	15.6	84.4	0
433	41.2	6.4	93.6	0
453	28.0	7.5	92.5	0
Over SZS catalyst				
413	42.7	12.6	75.6	11.7
433	52.1	3.3	86.4	10.4
453	43.2	0.4	64.6	35.0

acid sites catalyze dehydration of alcohols to olefins. However, Brønsted acid catalysis is not necessarily the sole cause of olefin formation. It has been shown that alcohols also can dissociatively adsorb on various metal oxides to form surface alkoxide intermediates ($*-OC_nH_m$)[12,13]; and these can then undergo further reaction to eliminate alkene. The details of the alkoxide pathway have been shown to depend on factors such as the structure[14] and the electronic nature[15] of the reacting alcohol. Lahousse, *et al.*[16] showed that catalytic redox ability is required for activity for dehydration of 2-propanol to propylene.

$$(CH_3)_2O \longrightarrow \longrightarrow *-OC_2H_5 \longrightarrow C_2H_4 \qquad (2)$$
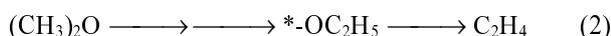
Formation of Propylene. Propylene was also formed as a secondary product over SZS, but not SZ (Table 3). Coupling of both carbon atoms from a single molecule of DME to form ethylene conceivably could have occurred by reaction at either one surface site or a small number of proximate sites. However, formation of propylene required participation of a third carbon atom, probably as a $*-CH_x$ (* represents a surface site) species, either from methanol or from a second molecule of DME (Eq. 3). Our argument is supported by the IR data (Figure 5) of spent SZS catalyst which shows a peak at 3013 cm^{-1} corresponding to CH bonding and a peak at 1593 cm^{-1} representing C=C bonding.

$$3CH_3OH \longrightarrow C_3H_6 + 3H_2O \qquad (3)$$
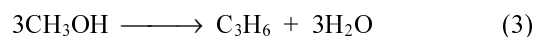
There has been debate as to whether ethylene is the only hydrocarbon product containing a C-C bond formed directly from DME or whether propylene should also be considered as directly formed from DME.[17,18] Two distinct mechanisms have been proposed. In the first mechanism, ethylene is initially formed *via* β-elimination from ethoxy species, and is subsequently methylated by reaction with a methoxy group (Eq. 4). Chain propagation proceeds *via* a methylation process. In the second mechanism, it has been suggested that methoxy groups interact with methanol and/or DME to form an iso-propoxy group, by a process analogous to that described for the formation of ethoxy species. Propylene then is formed by β-elimination from the isopropoxy species (Eq. 5). We suggest that the second propagation pathway is an essential feature of the mechanistic proposal of Van der

Berg, *et al.*[18]

$$CH_3OH \longrightarrow *-OCH_3$$
$$*-OC_2H_5 \longrightarrow C_2H_4 \rangle \longrightarrow *-OC_3H_7 \longrightarrow C_3H_6 \qquad (4)$$

$$(CH_3)_2O + *-OCH_3 \longrightarrow \longrightarrow *-OC_3H_7 \longrightarrow C_3H_6 \qquad (5)$$
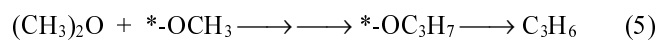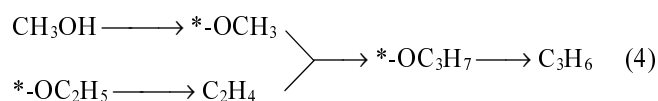
The present data provide further insight into the process, and suggest that intermediate surface species $*-CH_x$ were stabilized at highly acidic sites. The intermediate species then react with either C_2H_4, in a mechanism similar to Eq. (4), or with an intermediate such as an alkoxy species preceding formation of C_2H_4 (Eq. 6 a & b) to form the C_3 backbone of propylene.

$$CH_3OH \longrightarrow *-CH_x \qquad (6a)$$

$$*-OC_2H_5 + *-CH_x \longrightarrow *-OC_3H_7 \longrightarrow C_3H_6 \qquad (6b)$$
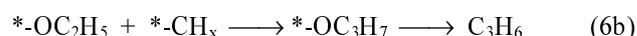
We proposed a mechanism in which a combination of pathway comprising parallel and consecutive reactions, involving nucleophilic and electrophilic species, is required for formation of DME, ethylene and propylene from methanol dehydration on acidic catalysts. In the present work, formation of propylene only occurred when surface sites had sufficiently high acidity to form $*-CH_x$ intermediate moieties, and these intermediates were themselves sufficiently reactive and proximate to react with $*-OC_2H_5$ intermediates and form the telomerized intermediate $*-OC_3H_7$. Thus, formation of propylene required that there was a high concentration of surface sites, and that several of these sites were highly acidic. SZS has a higher density and stronger multiple acidic sties than SZ. Thus, formation of propylene on SZS, and not on SZ, was consistent with the requirement that the more strongly acidic sites on SZS were available in high concentration for formation of C_3 surface intermediate species.

It is noteworthy that no hydrocarbon products higher than propylene were formed, even though the selectivity to propylene increased to 35% at 453 K over SZS. Three inferences can be drawn from these results.

First, there was no C_4 product, and so dimerization of C_2 intermediates or products does not occur to a detectable amount.

The second inference is that chain growth *via* only formation and assembly of C_1 intermediates probably was not a significant component of the mechanism. If the mechanism involved a significant amount of assembly of C_1 units to form the carbon backbone chain, it would be expected that the distribution of products would more closely resemble an Anderson-Schultz-Flory distribution. In that case, one would anticipate that a detectable amount of C_4 product also should have been formed when the selectivity to propylene was as high as 35%, but none was found. Thus, it is most probable that the mechanism involved reaction of a C_n species, most likely an alkoxy intermediate, with a $*-CH_x$ intermediate moiety to form a C_{n+1} chain, rather than assembly of the chain from only C_1 units.

The third inference is that if, indeed, the mechanism required chain growth through reaction of a C_n chain with *-CH$_x$ to form a C_{n+1} chain, then formation of a surface bonded C_4 intermediate was unfavoured. A limitation of this nature would be consistent with a mechanism in which the chain growth process occurred by nucleophilic attack at a secondary carbon in the present chain (C_nH_{2n} or *-OC$_n$H$_{2n+1}$) to form a branched product, and that there was steric constraint to formation of *-OC$_4$H$_9$ as a branched chain intermediate (Eq. 7).

$$\text{*OC}_3\text{H}_7 \text{ (or C}_3\text{H}_6) + \text{*-CH}_x \xrightarrow{\quad\quad} \text{*-OC}_4\text{H}_9 \qquad (7)$$
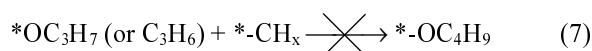
Apparent Rate Constants. Methanol conversion reaction data for all SZ and SZS catalyst tests were found to fit the Bassett-Habgood rate equation (Eq. 8) for first order reactions in which the reactant partial pressure is in the range 260-575 psig. The adsorption rate is faster than the rate of reaction, the latter being the rate-determining step.

$$\ln[1/(1-X)] = k_a RT(W/F) \qquad (8)$$

Where X is total conversion, k_a is the apparent rate constant, W is the weight of catalyst, and F is the weight of methanol in the reactor.

Plots of $\ln[1/(1-X)]$ Vs F^{-1} are linear for either SZ or SZS catalysts, and pass through the origin, as expected from Eq. (8). Therefore, the reaction is first order in methanol. Apparent rate constants, k_a, obtained from the slopes of the linear plots of $\ln[1/(1-X)]$ Vs F^{-1} and activation parameters calculated using the rate law equation (Eq. 8) are shown in Table 4.

Gas phase dehydration of alcohols to the corresponding olefins proceeds on acid catalysts *via* the reaction scheme presented in reference.[19] The mechanism proposed above proceeds *via* alkene elimination from surface alkoxy species.

The data obtained in this study are consistent with a mechanism of product formation that is substantially similar to that proposed for reaction in the gas phase.

On the basis of discussions presented above we proposed that Lewis and Brφnsted acid sites are in equilibrium on SZ and SZS, as shown in Eq. (9).

Dehydration of an alcohol to an alkene includes elimina-

$$\qquad (9)$$

Lewis Acid   Brφnsted Acid
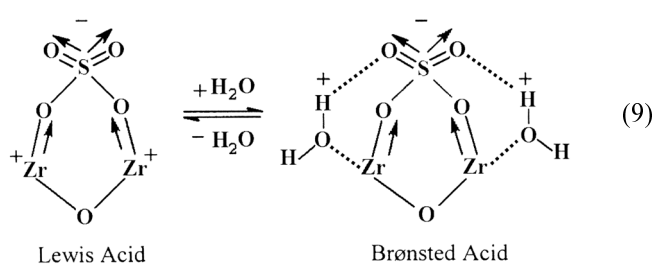
tion of the β-hydrogen atom from an adsorbed substrate. The nominally weak acidic OH groups in cation exchanged catalyst are sufficiently active to catalyze alcohol dehydration. Both SZ and SZS catalysts are more active for alcohol dehydration than other acid catalysts screened during a parallel study such as Zeolite 3A, Zeolite 5A dispersed on silica or alumina; sulfuric acid; Ce and Al phosphate catalysts dispersed on silica or alumina; Amberlyst 16 and Amberlyst 36 dispersed on silica or alumina, and alumina-silica catalysts having different alumina-silica ratios ranging between 20-80%.

Further reaction to form propylene occurred only over SZS. Thus, higher acidity and increased concentration of acidic sites on SZS compared to SZ enhanced activity for additional C-C bond formation reactions.

Correlation of Activity with Surface Properties. Doping of SZ with SiO_2 produced a SZS catalyst that was slightly more active for dehydrating methanol to dimethyl ether and ethylene than undoped SZ, and also produced propylene. A slight increase in selectivity to ethylene was also observed with SZS.

The TPD of pyridine adsorbed on SZS displayed features that characterized the presence of combinations of proximate acid sites in SZS, which were not present in TPD of pyridine on SZ. In addition, SZS was found to have a higher total acid site density, 2.4 mmol·m^{-2}, compared with 1.8 mmol·m^{-2} on SZ. Our study clearly indicates that concentrations of Brφnsted and Lewis acid sites determine catalytic activity and selectivity. Thus, the increase in catalytic activity of SZS compared to SZ, and the differences between the products obtained for the present reaction, were entirely consistent with the presence of a high concentration of proximate and strongly acidic sites only on SZS.

Sulfate Ion Leaching and Catalyst Stability. From Tables 1 and 2, it can be seen that the area, pore volume and crystallite size changed appreciably with use of either SZ or SZS as catalyst. However, the changes did not appear to affect catalytic activity or selectivity during a catalyst run. This indicated that the catalysts had acceptable physical stability over the duration of runs under the present experimental conditions.

Small amounts of sulfate ions and other oxyanion species within the catalyst phase were leached during the catalytic runs. The amount of sulfate leached from SZ (0.075 g (SO_4^{2-})/g(cat) and from SZS (0.025 g (SO_4^{2-})/g(cat) was determined by acid-base titration of the residual liquid reaction mixture. Leaching caused a significant change in crystallite size and, to a lesser degree, change in surface area.

Table 4. Apparent rate constants (k_a) and activation parameters (E_a and ln A) for methanol conversion on SZ and SZS catalysts, as derived from the Bassett-Habgood rate equation [20]

Temperature (K)	K_a (Apparent rate constant) (10^6 mol/atm.g.s.)	E_a (Activation energy) (kcal/mol)	ln A
SZ catalyst			
413	14.1	106 ± 3	−0.2
433	16.4	123 ± 4	0.6
453	12.0	100 ± 4	−1.8
SZS catalyst			
413	20.3	120 ± 3	−0.8
433	35.4	134 ± 4	1.4
453	18.7	110 ± 4	−2.0

Table 5. ^{1}H NMR of undoped and silica-doped sulfated zirconia, before and after pyridine (Py) adsorption

SZ				SZS				Remarks
Before Py ads.		After Py ads.		Before Py ads.		After Py ads.		
ppm	Intensity	ppm	Intensity	ppm	Intensity	ppm	Intensity	
		8.58^+	79.3^+			8.58^+	66.2^+	$^+$Pyridine peaks
		7.81^+	44.6^+			7.81^+	21.9^+	
		7.40^+	137.5^+			7.40^+	100.8^+	
5.75	62.9	5.75	13.4	5.75	151.0	5.75	48.4	*Solvent (DMSO) peaks
3.35^*	1050	3.35^*	1049	3.35^*	1046	3.35^*	1047	
2.51^*	260	2.51^*	250	2.51^*	258	2.51^*	261	
2.1	23.1	2.1	30.0	2.1	6.8	2.1	93.3	
1.2	9.6	1.2	9.6	1.2	2.4	1.9	30.4	
						1.2	2.9	

These data suggested that particles became aggregated during use. The amount of sulfate ions leached over the period of the experiments reported was not sufficient to induce any major change in the concentration or nature of catalyst sites on SZ and SZS catalysts during each run. The lesser amount of sulfate that was leached from SZS than from a same quantity of SZ showed that silica dopant increased the resistance of the catalyst to leaching.

Conclusion

Propylene was formed over sulfated zirconia doped with silica, but not over undoped sulfated zirconia. Formation of propylene is attributed to formation of intermediate *-CH$_x$ species at strongly acidic sites, which react with either ethylene, or with an alkoxy intermediate leading to formation of ethylene, in a chain propagation step. The catalytic activity and product selectivity show that doping sulfated zirconia with silica resulted in an increase in both acidity and concentration of surface acidic sites, and formation of proximate acid sites.

No hydrocarbon products higher than propylene were formed. This suggested that the mechanism proceeded *via* nucleophilic attack on the carbon chain of the intermediate, and that there was steric constraint to formation of branched C$_4$ or higher intermediates that would have been formed as a result of such a reaction.

The kinetics of ethylene formation are consistent with a β-elimination mechanism from a surface intermediate alkoxy species derived from methanol.

Sulfated zirconia doped with silica was more stable than undoped catalyst, and less prone to leaching of sulfate.

FTIR, NMR and pyridine adsorption showed that doping sulfated zirconia with silica resulted in an increase in both acidity and concentration of Brϕnsted acid sites, and formation of proximate acid sites.

Correlation of spectroscopic data with differences between reaction data for dehydration of methanol to dimethyl ether, ethylene and propylene over the doped and undoped

catalysts showed that the highly acidic sites were related to the higher catalytic activity of the doped catalyst.

Formation of propylene over sulfated zirconia doped with silica, but not over undoped sulfated zirconia, was attributed to formation of intermediate CH$_x$ species at strongly acidic sites. Differences between the combination and relative strengths of Lewis, Brϕnsted and complex proximate acid sites on the surfaces of undoped sulfated zirconia and sulfated zirconia doped with silica determined their relative catalytic activity and selectivity.

References

1. Baiker, A.; Kijenski, J. *Catal. Today* **1989**, *5*, 1.
2. Hino, M.; Kobayashi, M.; Arata, K. *J. Am. Chem. Soc.* **1986**, *108*, 6439.
3. Kung, H. H. *Solid State Chem.* **1984**, *52*, 191.
4. Tanabe, K.; Sumiyoshi, T.; Shibata, K.; Kiyoura, T. *Bull. Chem. Soc. Jpn.* **1974**, *47*, 1064.
5. Tanabe, K.; Itoh, M.; Morishige, K.; Hattori, H. in *Preparation of Catalysts*; Delmon, B.; Jacobs, P. A.; Poncelet, G., Eds.; Elsevier: Amsterdam, 1976; p 65.
6. Arata, K. *Adv. Catal.* **1990**, *37*, 165.
7. Corma, A. *Chem. Rev.* **1995**, *95*, 559.
8. Willams, C.; Makarova, M. A.; Malysheva, L. V.; Paukshits, E. A.; Thomas, J. M.; Zamaraev, K. I. *J. Chem. Soc. Farady Trans.* **1990**, *86*, 3473.
9. Kanazirev, V.; Tsoncheva, T. *Minchev, Chr, Z. Phys. Chem. N.F.* **1986**, *149*, 237.
10. Tanabe, K.; Misono, M.; Ono, Y.; Hattori, H. In *New Solid Acids and Bases, Their Catalytic Properties*; Delmon, B.; Yates, J. T., Eds.; Elsevier: Amsterdam, 1989; Vol. 51.
11. Gervasini, A.; Auroux, A. *J. Catal.* **1991**, *131*, 190.
12. Vohs, J. M.; Barteau, M. A. *Surf. Sci.* **1989**, *221*, 5909.
13. Vohs, J. M.; Barteau, M. A. *J. Phys. Chem.* **1991**, *95*, 227.
14. Cunningham, J.; Hodnett, B. K.; Illyas, M.; Tobin, J.; Leahy, E. L.; Fierro, J. L. G. *Discuss. Farady Soc.* **1981**, *72*, 283.
15. Parrot, S. L.; Rogers, Jr. J. W.; White, J. M. *Appl. Surf. Sci.* **1978**, *1*, 443.
16. Lahousse, C.; Bachelier, J.; Lavally, J. C.; Lauron-Pernot, H.; LeGovie, A. M. *J. Mol. Cata.* **1994**, *87*, 329.
17. Kannan, S. V.; Pillai, C. N. *Curr. Sci.* **1968**, *23*, 665.
18. Bassett, D.; Habgood, H. W. *J. Phys. Chem.* **1960**, *64*, 769.
19. Buchang, S.; Burton, H. D. *J. Catal.* **1995**, *57*, 359.